Low-temperature magnetic properties and high-temperature diffusive behavior of $LiNiO_2$ investigated by muon-spin spectroscopy

Jun Sugiyama,[1,*] Yutaka Ikedo,[2] Kazuhiko Mukai,[1] Hiroshi Nozaki,[1] Martin Månsson,[3] Oren Ofer,[4] Masashi Harada,[1] Kazuya Kamazawa,[1] Yasuhiro Miyake,[2] Jess H. Brewer,[4,5] Eduardo J. Ansaldo,[4] Kim H. Chow,[6] Isao Watanabe,[7] and Tsutomu Ohzuku[8]

[1]*Toyota Central Research and Development Laboratories Inc., Nagakute, Aichi 480-1192, Japan*

[2]*Muon Science Laboratory, Institute of Materials Structure Science, KEK, 1-1 Oho, Tsukuba, Ibaraki 305-0801, Japan*

[3]*Laboratory for Neutron Scattering, ETH Zürich and Paul Scherrer Institut, CH-5232 Villigen PSI, Switzerland*

[4]*TRIUMF, 4004 Wesbrook Mall, Vancouver, British Columbia, Canada V6T 2A3*

[5]*Department of Physics and Astronomy, University of British Columbia, Vancouver, British Columbia, Canada V6T 1Z1*

[6]*Department of Physics, University of Alberta, Edmonton, Alberta, Canada T6G 2G7*

[7]*Muon Science Laboratory, RIKEN, 2-1 Hirosawa, Wako, Saitama 351-0198, Japan*

[8]*Department of Applied Chemistry, Graduate School of Engineering, Osaka City University, Osaka 558-8585, Japan*

(Received 26 September 2010; published 10 December 2010)

In order to elucidate the effect of Ni ions in the Li layer on magnetism and Li diffusion of $LiNiO_2$, we have measured muon-spin rotation and muon-spin relaxation (μ^+SR) spectra for the polycrystalline $Li_{1-x}Ni_{1+x}O_2$ samples with $x=0.02$, 0.03, and 0.15. Weak transverse-field-μ^+SR measurements demonstrated the existence of a bulk ferromagnetic transition at $T_m=48(6)$ K for the $x=0.03$ sample and 161(7) K for $x=0.15$ while the $x=0.02$ sample exhibited an antiferromagnetic transition at 18(4) K. Zero-magnetic-field-(ZF) μ^+SR measurements below T_m clarified the formation of static ferromagnetic (FM) order for the $x=0.03$ and 0.15 samples but only a highly disordered antiferromagnetic (AF) order for the $x=0.02$ sample. Therefore, the variation in the low-T magnetism with x is most unlikely due to the change in the concentration of an AF NiO-type domain or an FM Ni-rich cluster but likely due to a homogeneous change in the whole system. In the paramagnetic state, ZF- and longitudinal-field-μ^+SR spectra exhibited a dynamic nuclear field relaxation. From the temperature dependence of the field fluctuation rate, a diffusion coefficient of Li^+ ions (D_{Li}) at 300 K was estimated about $0.39(3)\times10^{-11}$ cm^2/s for the $x=0.02$ sample and $0.12(7)\times10^{-11}$ cm^2/s for $x=0.15$. On the other hand, the related compound, $LiCrO_2$, did not show any diffusive behavior even at the highest temperature measured (=475 K). Considering the hindrance of diffusion by Ni in the Li^+ diffusion plane and the fact that $LiCrO_2$ is electrochemically inactive, the estimated D_{Li} is thought to be very reasonable for the positive electrode material of Li-ion batteries. Furthermore, at low temperatures where the Li^+ ions are static, the internal magnetic field was still found to be fluctuating, due to a dynamic local Jahn-Teller distortion of the Ni^{3+} ions in a low-spin state with $S=1/2(t_{2g}^6e_g^1)$.

DOI: 10.1103/PhysRevB.82.224412 PACS number(s): 76.75.+i, 66.30.H−, 82.47.Aa, 82.56.Lz

I. INTRODUCTION

Diffusion of Li^+ ions in solids is a basic principle behind the operation of Li-ion batteries. Such diffusive behavior is represented by the diffusion equation (Fick's law), $J=-D\times\partial\phi/\partial x$, where J is the diffusion flux, D is the diffusion coefficient, ϕ is the concentration, and x is the position. Although D of Li^+ ions (D_{Li}) in solids is usually evaluated by ^{7}Li-NMR, difficulties arise for materials that contain magnetic ions. This is because the magnetic ions contribute additional spin-lattice relaxation processes that is considerably larger than the $1/T_1$ expected from only Li diffusion.[1,2] In fact, D_{Li} estimated by ^{7}Li-NMR for $LiCoO_2$ and $LiNiO_2$ (Ref. 3) is known to be three or four order of magnitude smaller than the D_{Li} predicted by first-principles calculations.[4] This implies that ^{7}Li-NMR provides a very rough estimate of D_{Li} for the positive electrode materials of Li-ion batteries, which include transition-metal ions in order to compensate charge neutrality during a Li^+ intercalation/deintercaltion reaction. This is a highly unsatisfactory situation since D_{Li} is one of the primary parameters that govern the charge/discharge rate of a Li-ion battery, particularly a future solid-state battery.

We have, therefore, attempted to measure D_{Li} for lithium transition-metal oxides with muon-spin relaxation (μ^+SR) since 2005,[5–7] although there were a few μ^+SR reports on lithium transition-metal oxides, i.e., $LiMn_2O_4$ spinel[8,9] and $Li_{0.6}TiO_2$.[10] Muons do not feel fluctuating magnetic moments at high T but instead sense the change in nuclear dipole field due to Li diffusion. Even if magnetic moments still affect the muon-spin depolarization rate, such an effect is, in principle, distinguishable from that of nuclear dipole fields. In particular, a weak longitudinal field can be applied that decouples the magnetic and nuclear dipole interactions.[11,12] (Here, "longitudinal field" means a magnetic field is applied parallel to the initial muon-spin polarization.)

In Li_xCoO_2, as T increases from 50 K, the field fluctuation rate (ν) is initially constant (eventually 0), but starts to increase above 160 K,[7] around which the ^{7}Li-NMR line width suddenly decreases due to a motional narrowing.[13] Furthermore, the T dependence of ν was well explained by a thermal activation process in the T range between 160 and 250 K. Assuming a random-walk jump of the Li^+ ions between the neighboring sites, D_{Li}(300 K) for $Li_{0.73}CoO_2$ is estimated as about 13.3×10^{-11} cm^2/s,[7] which is comparable to the pre-

diction from first-principles calculations.[4] In order to further confirm the unique power of μ^+SR for detecting D_{Li} in solids, it is definitely necessary to measure D_{Li} for other materials by means of μ^+SR.

In this paper, we select $LiNiO_2$ and related materials as a target because they have been heavily investigated as a positive electrode material for the next-generation Li-ion batteries.[14–20] In the rhombohedral $LiNiO_2$ lattice with space group $R\bar{3}m$, the NiO_2 plane and the Li layers form alternating stacks along the c_H axis in the hexagonal setting.[21] In the NiO_2 planes, Ni ions form a two-dimensional triangular lattice (2DTL) by a network of edge-sharing NiO_6 octahedra. Since the Ni^{3+} ions are in a low-spin state with $S=1/2$, $LiNiO_2$ was proposed to be an ideal half-filled 2DTL.[22] In contrast to $LiCoO_2$, stoichiometric $LiNiO_2$ has never been prepared so far.[23,24] That is, the excess Ni is usually present in the Li layer of the $LiNiO_2$ samples due to the similarity in ionic radii between Li^+ and Ni^{3+}.[25–27] The ionic distribution of the Ni-excess $LiNiO_2$ is, thus, given by $(Li^+_{1-x}Ni^{2+}_x)_{3b}[Ni^{2+}_xNi^{3+}_{1-x}]_{3a}O_2$,[26] where $3b$ and $3a$ are the Li and Ni site in the regular $LiNiO_2$ lattice. Since the $(Ni^{2+})_{3b}$ ions introduce an additional ferromagnetic (FM) interaction between the adjacent NiO_2 planes,[28] the magnetic nature of $Li_{1-x}Ni_{1+x}O_2$ strongly depends on x.[25–27,29] In fact, the reason why long-range AF order does not exist for nearly stoichiometric $LiNiO_2$ (Refs. 30–32) was clearly explained by the effect of the $(Ni^{2+})_{3b}$ ions by recent μ^+SR study of the $x \leq 0.03$ compound.[33,34] More correctly, the magnetic ground state of nearly stoichiometric $LiNiO_2$ is found to be a "static but short range." A-type antiferromagnetic (AF) ordered system, in which the Ni^{3+} moments align ferromagnetically along the c_H axis in the NiO_2 plane with an incommensurate modulation due to canting of the Ni^{3+} moments but align antiferromagnetically between adjacent NiO_2 planes. However, the x dependence of microscopic magnetism of $Li_{1-x}Ni_{1+x}O_2$ was not investigated by μ^+SR so far, although the change with x is thought to occur very locally.

Besides the interesting change in the low-T magnetism of $Li_{1-x}Ni_{1+x}O_2$ with x, the $(Ni^{2+})_{3b}$ ions are naturally expected to reduce D_{Li} at high T,[19,20,35] because of the hindrance of diffusion by $(Ni^{2+})_{3b}$ in the Li^+ diffusion plane, in which Li^+ ions move relatively easily. Nevertheless, there is less systematic work on the relationship between D_{Li} and x while the charge/discharge performance was studied as a function of x.[19,35] The μ^+SR experiment on $Li_{1-x}Ni_{1+x}O_2$ with $x \geq 0$, therefore, provides crucial information on the effect of x on both magnetism and D_{Li}, resulting in clear insight regarding how to improve cathode materials.

II. EXPERIMENT

A powder sample of $LiNiO_2$ was prepared by a solid-state reaction technique using reagent grade $LiNO_3$ and $Ni(NO_3)_2$ powders as starting materials. A mixture of the two powders was well mixed with a mortar and pestle, then pressed into a pellet of 23 mm diameter and 5 mm thickness. The pellet was heated at 650 °C for 12 h in an air flow, and then ground and pressed into a pellet again. Then, the pellet was annealed for 12 h in an oxygen flow at 750 °C. In order to increase x in $Li_{1-x}Ni_{1+x}O_2$, the pellet heated at 650 °C was also annealed for 12 h in an oxygen flow at 850 or 950 °C.

TABLE I. Structural, compositional, and magnetic properties of the three $LiNiO_2$ samples prepared with different annealing temperatures; (top) lattice parameters obtained by the analysis of the synchrotron XRD data using a Rietveld technique (upper middle) chemical compositions determined by an ICP-AES analysis (lower middle) Curie-Weiss parameters obtained by susceptibility measurements, and (bottom) a bulk magnetic transition temperature detected by weak transverse field μ^+SR measurements. Here, the lattice parameters were calculated for the hexagonal unit cell. x_{XRD} was evaluated from the occupancies of Li and Ni at the $3b$ site, while x_{ICP} is converted from the Li/Ni ratio by the relation $x=(1-y)/(y+1)$, where y=Li/Ni. Due to the presence of the Li_2CO_3 phase in the three samples, x_{ICP} is naturally smaller than the amount of Ni ions at the $3b$ site for both samples. Thus, x_{XRD} is used for the composition of the present $Li_{1-x}Ni_{1+x}O_2$ phase.

Annealing T (°C)	750	850	950
a_H (nm)	0.28784(1)	0.28831(1)	0.28955(1)
c_H (nm)	1.41963(2)	1.42037(2)	1.42309(2)
x_{XRD}	0.019	0.027	0.154
Li/Ni	1.01(1)	0.93(1)	0.87(1)
x_{ICP}	−0.005(5)	0.036(5)	0.070(6)
Θ_{CW} (K)	40.8(5)	90.8(1.4)	166(6)
μ_{eff} (μ_B)	2.14(1)	1.91(1)	1.50(4)
T_m (K)	18(4)	48(6)	161(7)

Powder x-ray diffraction (XRD) patterns for the three samples were measured on BL02B2 of SPring-8 in Japan with wavelength $\lambda_{x\ ray}=1.00081(1)$ Å. According to a Rietveld analysis using a computer program RIETAN2000,[36] the three samples were assigned as almost a single phase of a rhombohedral symmetry with space group $R\bar{3}m$ together with a small amount of Li_2CO_3 phase, as already reported.[35] The composition of the samples were checked by an inductively coupled plasma-atomic emission spectral (ICP-AES) (CIROS 120, Rigaku Co. Ltd., Japan) analysis. The results of the XRD and ICP-AES analyses were summarized in Table I.

In order to estimate the excess Ni in the Li plane, χ was measured below 400 K under a $H \leq 10$ k Oe field with a superconducting quantum interference device magnetometer (MPMS, Quantum Design). The Weiss temperature (Θ_{CW}) and effective magnetic moment (μ_{eff}) were determined from the T dependence of susceptibility (χ) by fitting to a Curie-Weiss (CW) law, $\chi=C/(T-\Theta_{CW})$ and $C=(Ng^2\mu_B^2/3k_B)\mu_{eff}^2$ in the T range between 80 and 400 K. Here, N is the number density of Ni spins, g is the Landé g factor, μ_B is the Bohr magneton, and k_B is Boltzmann's constant. As a result, we obtained $\Theta_{CW}=40.8\pm0.5$ K and $\mu_{eff}=2.14\pm0.01$ μ_B, respectively [see Figs. 1(a) and 1(b)], assuming that $g=2$.[37] In addition, the $\chi(T)$ curve obtained with $H=100$ Oe exhibits a clear cusp at 11 K ($=T_m$), as seen in Fig. 3(c). Since these values are in good agreement with those reported for $Li_{1-x}Ni_{1+x}O_2$ with $x \leq 0.02$ (Refs. 23, 25, 29, and 37) and our previous result,[33] x for the sample annealed at 750 °C is determined as ~0.02. The composition of the samples annealed at 850 °C and 950 °C are determined as $x=0.03$ and

$x=0.15$, respectively, based on the XRD analysis.

The μ^+SR spectra were measured at the surface muon beam lines using the LAMPF spectrometer of TRIUMF in Canada, the ARGUS spectrometer of ISIS/Riken-RAL in U.K., and the D-OMEGA1 spectrometer of MUSE/MLF/J-PARC in Japan. In TRIUMF, the approximately 500 mg powder sample was placed in an envelope with 1×1 cm^2 area, which is made of very thin Al-coated Mylar tape, and then the envelope was attached to a low-background (BG) sample holder in a liquid-He flow-type cryostat in the T range between 1.8 and 250 K. In Riken-RAL and J-PARC, on the other hand, a ~2 g powder sample was pressed into a disk with 27 mm diameter and 1 mm thickness, and packed into an Au-O ring sealed titanium cell. The window of the cell was made of a Kapton film with 50 μm thickness. The cell was mounted onto the Cu plate of a liquid-He flow-type cryostat in the T range between 10 and 500 K. The experimental techniques are described in more detail elsewhere.[12]

III. RESULTS

A. Magnetization below 400 K

Prior to the μ^+SR results, we at first show the results of the magnetization measurements. Figure 1(a) shows the T dependence of χ for the $x=0.02$, 0.03, and 0.15 samples. As T decreases from 400 K, the $\chi(T)$ curve exhibits a sudden increase below $\sim$60 K for the $x=0.02$ sample, below $\sim$100 K for $x=0.03$ and below $\sim$200 K for $x=0.15$. According to the $\chi^{-1}(T)$ curve [Fig. 1(b)], these samples are a CW paramagnet at high temperatures. In fact, a CW fit in the T range between 200 and 400 K for the $x=0.03$ sample (between 320 and 400 K for $x=0.15$) yielded $\Theta_{CW}=90.8\pm1.4$ K and $\mu_{eff}=1.91\pm0.01$ μ_B (166 ± 6 K and 1.50 ± 0.04 μ_B). This means that FM interaction increases with x, being consistent with the fact that the $(Ni^{2+})_{3b}$ ions introduce an additional FM interaction between the adjacent NiO_2 planes, regardless with the sign of the interaction between $(Ni^{2+})_{3b}$ and $(Ni)_{3a}$.[28] This is confirmed by the relationship between magnetization (M) and H for the $x\geq0.03$ samples [Fig. 1(c)]. The $M(H)$ curve shows an FM behavior for the $x=0.03$ and 0.15 samples at 5 K, being consistent with the past work.[29,38] Note that, the value of M at the highest H measured (=55 k Oe) for the $x=0.15$ sample is almost the same to those for the $x=0.03$ and even for $x=0.02$ samples, despite the increase in Θ with x.

On the other hand, μ_{eff} is found to decrease with x, as reported in the past work.[29] However, it is difficult to explain this behavior using the assumption that the Ni^{2+} ions are in an $S=1(t_{2g}^6e_g^2)$ state. This is because, since the Ni^{3+} ions are in an $S=1/2(t_{2g}^6e_g^1)$ state,[39] μ_{eff} is expected to increase with x. This discrepancy could be explained by the hypothesis that the highest T measured (=400 K) is too low to obtain a pure CW behavior.[35]

B. Low-temperature magnetic properties

1. Weak transverse field μ^+SR

In order to study the effect of x on the microscopic magnetic nature of $Li_{1-x}Ni_{1+x}O_2$, we initially measured μ^+SR spectra in a weak transverse field (wTF=50 Oe). Here, "weak" means that the applied field is significantly less than any possible spontaneous internal fields (H_{int}) in the ordered state. The wTF-μ^+SR technique is sensitive to local magnetic order via the decrease in the amplitude (asymmetry) of the μ^+ spin precession signal and the enhanced μ^+ spin relaxation. Figure 2 shows the variation in the wTF time spectra of $Li_{0.85}Ni_{1.15}O_2$ at different temperatures. When T decreases below $\sim$160 K, the oscillation amplitude due to wTF rapidly decreases, indicating the appearance of additional strong H_{int}. At 130 K, the wTF oscillation eventually disappears and the spectrum consists of a fast relaxing signal in an early time domain and a slowly relaxing tail signal. The wTF-μ^+SR spectrum was consequently fitted using a combination of a slowly relaxing precessing signal and two exponentially relaxing nonoscillatory signals. The first component is due to the externally applied magnetic field (wTF =50 Oe) and the second and third are due to H_{int}.

$$A_0P_{TF}(t)=A_{TF}\cos(\omega_{TF}^{\mu}t+\phi_{TF})\exp[-(\lambda_{TF}t)^{\beta}]+A_{fast}\exp(-\lambda_{fast}t)+A_{slow}\exp(-\lambda_{slow}t), \quad (1)$$

where A_0 is the initial ($t=0$) asymmetry, $P_{TF}(t)$ is the muon-spin-polarization function, ω_{TF}^{μ} is the muon Larmor frequency corresponding to the applied wTF, ϕ_{TF} is the initial phase of the precessing signal, λ_{TF}, λ_{fast}, and λ_{slow} are the exponential relaxation rates, and A_{TF}, A_{fast}, and A_{slow} are the asymmetries of the three components of the μ^+SR spectrum.

By plotting A_{TF} versus T [see Fig. 3(a)], we can clearly see that the $x=0.15$ sample has a bulk magnetic transition at $T_m=161\pm7$ K, where the normalized $A_{TF}(=A_{TF}/A_0=N_{A_{TF}})=0.5$. This is because the normalized A_{TF} corresponds to the volume fraction of paramagnetic (PM) phases in a sample. For the $x=0.03$ ($x=0.02$) sample, T_m is estimated as 48 ± 6 K(18 ± 4 K). As T decreases from 250 K, the $\lambda_{TF}(T)$ curve exhibits a critical behavior toward T_m for the three samples [Fig. 3(b)], as expected. Moreover, since the normalized A_{TF} reaches 0 below the vicinity of T_m for the three samples, the volume fraction of the Li_2CO_3 phase in the samples is negligibly small, i.e., below a few percent. The A_{slow} component is the "1/3 tail" due to the quasistatic internal fields, as discussed later for the zero-magnetic field (ZF) data.

On the other hand, the $\chi(T)$ curve shows the appearance of a spontaneous magnetization for the $x=0.03$ and 0.15 samples at T_m, due to an FM transition while that of $Li_{0.98}Ni_{1.02}O_2$ shows a cusp at 11 K. Here, the μ^+SR and χ results on $Li_{0.98}Ni_{1.02}O_2$ are reproducible to our previous work.[33] Note that it is difficult to judge whether the whole volume of the sample enters into a magnetic phase, based only on the $\chi(T)$ curve. We, therefore, wish to emphasize that the present wTF-μ^+SR measurements clearly demonstrates the existence of a bulk FM transition at T_m for $Li_{1-x}Ni_{1+x}O_2$ with $x=0.03$ and 0.15. It is also very interesting that only 3% Ni ions in the Li layer [$(Ni^{2+})_{3b}$ ions] is sufficient to induce an FM transition in the whole sample. Such a $(Ni^{2+})_{3b}$ ion was previously believed to produce a localized magnetic ordered region in its vicinity. The present result, therefore, suggests that the $(Ni^{2+})_{3b}$ ion not only mediates the

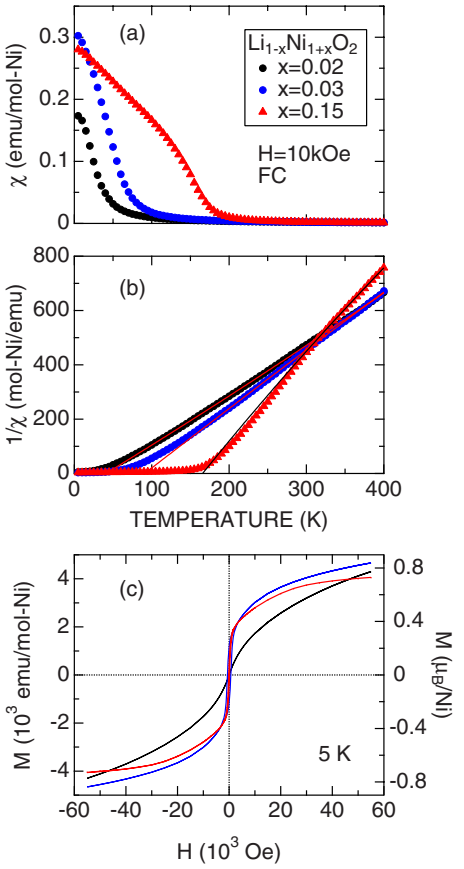

FIG. 1. (Color online) T dependence of (a) susceptibility (χ) and (b) $1/\chi$, and (c) the relationship between magnetization (M) and magnetic field (H) at 5 K for $Li_{1-x}Ni_{1+x}O_2$ with x=0.02, 0.03, and 0.15. The χ data were obtained in field cooling (FC) mode with H=10 kOe. Solid lines in (b) represent a linear fit in the T range between 80 and 400 K for the x=0 sample (between 200 and 400 K for x=0.03 and between 320 and 400 K for x=0.15) using a Curie-Weiss formula.

local FM order between the adjacent NiO_2 planes but also strongly reduces the AF coupling between them. This is consistent with the fact that long-range A-type AF order was not detected so far even for the most stoichiometric $LiNiO_2$ sample prepared.[23,24]

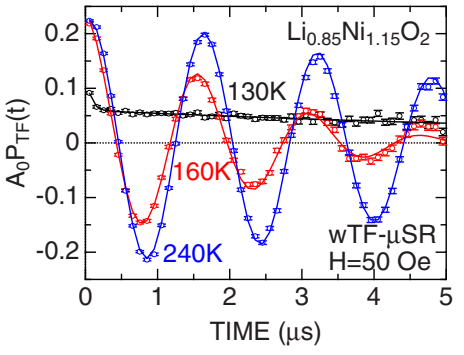

FIG. 2. (Color online) T dependences of the weak transverse field spectrum for $Li_{0.85}Ni_{1.15}O_2$. These spectra were obtained in TRIUMF.

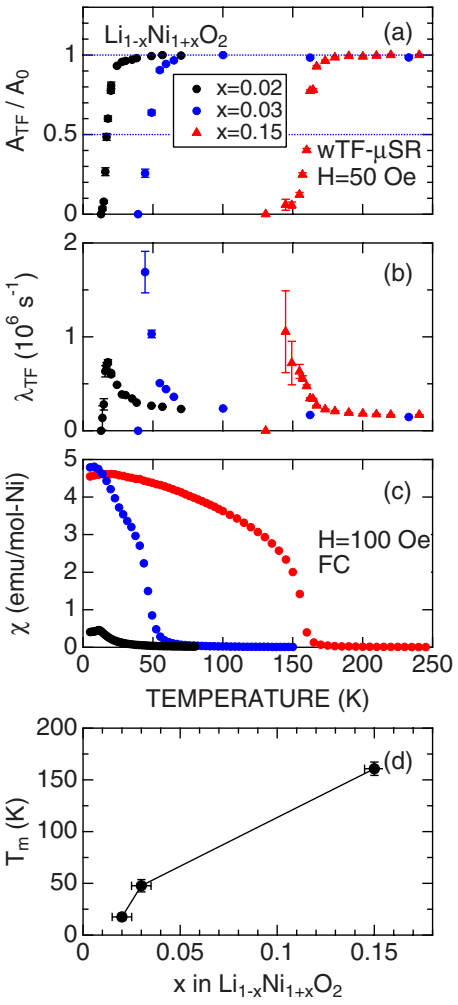

FIG. 3. (Color online) T dependences of (a) normalized weak transverse field asymmetry (A_{TF}/A_0), (b) relaxation rate (λ_{TF}), and (c) susceptibility (χ) obtained in FC mode with H=100 Oe for $Li_{1-x}Ni_{1+x}O_2$ with x=0.02, 0.03, and 0.15.

Figure 3(d) shows the relationship between T_m and x for $Li_{1-x}Ni_{1+x}O_2$. Since the other end compound with x=1, i.e., NiO, is known to be an antiferromagnet with T_N=523 K,[40] the magnetic phase diagram of the $Li_{1-x}Ni_{1+x}O_2$ system is likely very complex. Furthermore, we wish to point out that the present μ^+SR results excludes the scenario, in which the amount of the NiO-type domain increases with x.[41] This is because, if such scenario is correct, the volume fraction of the magnetic phase is expected to increase with x but T_m should not change with x. For the same reason, the FM-cluster model, in which the amount of an FM Ni-rich cluster increases with x,[35,37] is also most unlikely correct. The variation in the magnetic nature for $Li_{1-x}Ni_{1+x}O_2$ with x is, on the contrary, considered to be caused by a homogeneous change in the whole system.

2. Zero field μ^+SR

In order to further elucidate the nature of the magnetic phase, we measured the μ^+SR spectra in ZF for the three samples. The ZF μ^+SR technique is uniquely sensitive to

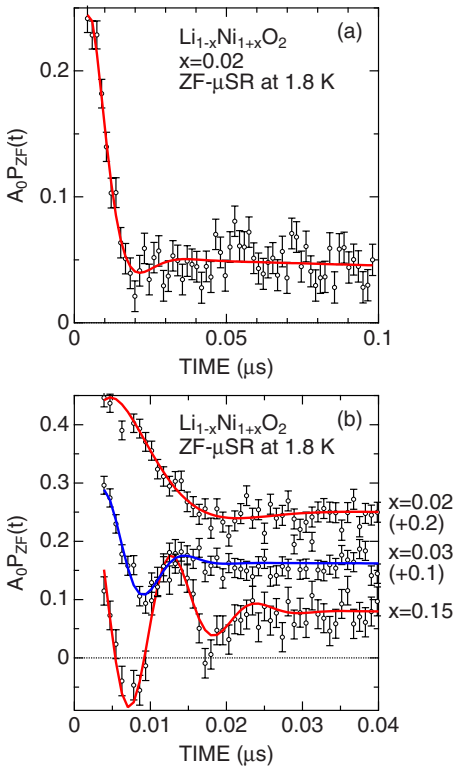

FIG. 4. (Color online) The ZF-μ^+SR time spectra at the lowest T measured for the three $Li_{1-x}Ni_{1+x}O_2$ samples; (a) only for the $x=0.02$ sample in the time window between 0 and 0.1 μs, and (b) for the $x=0.02$, 0.03, and 0.15 samples from top in the time window between 0 and 0.04 μs. Solid lines represent the fitting result using Eqs. (2) and (3). Each spectrum is offset by 0.1 for clarity of display. These spectra were obtained in TRIUMF.

local magnetic [dis]order in samples exhibiting quasistatic paramagnetic moments. Figure 4 shows their ZF spectra in an early time domain at the lowest T measured (=1.8 K). For the $x=0.02$ sample, the ZF spectrum shows only a first broad minimum around 0.2 μs. The spectrum was well fitted by a combination of the Bessel function $[J_0(\omega t)]$ and two exponentially relaxing nonoscillatory signals

$$A_0P_{ZF}(t) = A_{AF}J_0(\omega_{AF}t)\exp(-\lambda_{AF}t) + A_{fast}\exp(-\lambda_{fast}t) + A_{slow}\exp(-\lambda_{slow}t). \quad (2)$$

The former corresponds to the signal that muons "see" the incommensurate or widely distributed magnetic field[12,42] caused by a small amount of the $(Ni^{2+})_{3b}$ ions and the latter two nonoscillatory signals correspond to the 1/3 "tail" signal. These behavior are the same to those for the $x<0.03$ compound, previously reported.[33] Although $J_0(\omega t)$ is widely used for fitting the ZF-μ^+SR spectrum in an incommensurate AF ordered state, it should be noted that $J_0(\omega t)$ only provides a wide distribution of an internal magnetic field. Even for a commensurate AF ordered state, the ZF spectrum would be fitted by $J_0(\omega t)$, when the spectrum consists of multiple signals with different muon-spin precession frequencies.[43]

On the other hand, the ZF spectra for the $x=0.03$ and 0.15 samples show a clear oscillation, although they are rapidly relaxing. The ZF spectra for the both samples were well fitted by a combination of the Gaussian relaxing cosine oscillation for the static internal field and two exponentially relaxing signals

$$A_0P_{ZF}(t) = A_{FM}\cos(\omega_{FM}^{\mu}t + \phi_{FM})\exp\left(-\frac{\sigma_{FM}^2t^2}{2}\right) + A_{fast}\exp(-\lambda_{fast}t) + A_{slow}\exp(-\lambda_{slow}t), \quad (3)$$

where A_0 is the initial asymmetry and A_{FM}, A_{fast}, and A_{slow} are the asymmetries associated with the three signals. $\omega_{FM}^{\mu}(\equiv 2\pi f)$ is the muon Larmor frequency corresponding to the static internal FM field, ϕ_{FM} is the initial phase of the precessing signal, σ_{FM}, λ_{fast}, and λ_{slow} are the Gaussian and exponential relaxation rates of the three signals. Here, the total asymmetry is fixed as 0.24, i.e., $\Sigma A_i = A_0 = 0.24$, which was determined by the wTF measurements above T_m.

Figure 5 shows the T dependences of the ZF-μ^+SR parameters for the three samples. Here, the data for the $x=0.02$ sample is the same to those in Ref. 33, i.e., the wTF result and the ZF spectrum at 1.8 K for the present $x=0.02$ sample are the same to those for the previous sample. The fit for the ZF spectrum at 1.8 K using Eq. (3) yields $\phi_{FM}=7.1\pm0.4°(11.5\pm0.1°)$ for the $x=0.03(0.15)$ sample, i.e., eventually $\phi_{FM}=0$. This indicates that the spin structure of the $x=0.03$ and 0.15 samples is commensurate to the lattice, in contrast to $Li_{0.98}Ni_{1.02}O_2$.

The $f(T)$ curve [Fig. 5(a)] exhibits an order-parameterlike T dependence. That is, as T decreases from T_m, which is indicated by the arrow on the horizontal axis, f increases monotonically down to the lowest T measured with decreasing the slope (df/dT). Furthermore, as expected from Fig. 4, $f(T\rightarrow 0)$ for the $x=0.15$ sample is almost the same to that for the $x=0.03$ sample ($\sim$90 MHz). This means that the internal FM field at the muon site does not vary with x for the samples with $x\geq 0.03$, although T_m clearly depends on x. This behavior is consistent with the results of the magnetization measurements. That is, according to the $M(H)$ curve [Fig. 1(c)], the saturated magnetization per Ni ions for the $x=0.03$ sample is comparable to that for the $x=0.15$, indicating that the FM internal field of each domain, which muons sense, does not depend on x for samples with $x\geq 0.03$.

The relaxation rate σ_{FM} also increases with decreasing T, and then levels off around 60×10^6 s^{-1}(100×10^6 s^{-1}) below 140 K (35 K) for the $x=0.15$ (0.03) sample, although the data for the $x=0.03$ sample is scattering. However, σ_{FM} is likely to decrease with x, as clearly seen in Fig. 4. Finally, as T decreases from T_m, the normalized FM asymmetry (A_{FM}/A_0) increases, and then levels off around 0.7 below 120 K (35 K) for the $x=0.15$ (0.03) sample. Considering the 1/3 tail component, this indicates that the whole volume of the sample enters into an FM ordered phase.

For the $x=0.15$ sample, A_{slow}/A_0 is almost T independent ($\sim$1/3) in the whole T range below T_m while A_{fast}/A_0 is nonzero only below the vicinity of T_m [Fig. 5(d)]. Considering the magnitude of $A_{FM}/A_0(\sim 2/3)$ below T_m and a very small magnitude of λ_{slow} and λ_{fast} compared with σ_{FM}, both

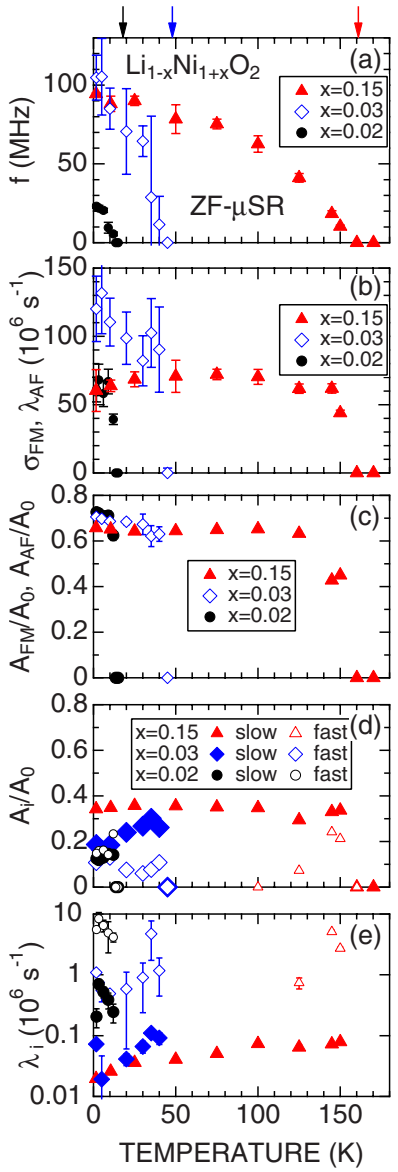

FIG. 5. (Color online) T dependences of ZF-μ^+SR parameters for the $Li_{1-x}Ni_{1+x}O_2$ samples with x=0.02, 0.03, and 0.15; (a) muon-spin precession frequency ($f=\omega_{FM}^{\mu}/2\pi$), (b) the relaxation rate (σ_{FM} and λ_{AF}), (c) the normalized asymmetry for the oscillatory signal (A_{FM}/A_0 and A_{AF}/A_0), (d) the normalized asymmetry for the nonoscillatory signals (A_i/A_0), and (e) their relaxation rates (λ_i). The data were obtained by fitting the ZF spectra using Eqs. (2) and (3). Arrows on the top horizontal axis of (a) show T_m determined by the wTF measurements. Symbols in (e) are the same to those in (d).

A_{slow} and A_{fast} signals are assigned as the 1/3 tail signal. For the other two samples, although A_{fast}/A_0 poses a nonzero value even at the lowest T measured, the overall behavior of the nonoscillatory signals is reasonable for the 1/3 tail signal, as well as that for the x=0.15 sample.

C. High-temperature diffusive behavior

1. Zero- and longitudinal-field μ^+SR

In the paramagnetic state above T_m, the ZF-μ^+SR spectrum exhibits a slow relaxation due to a nuclear magnetic

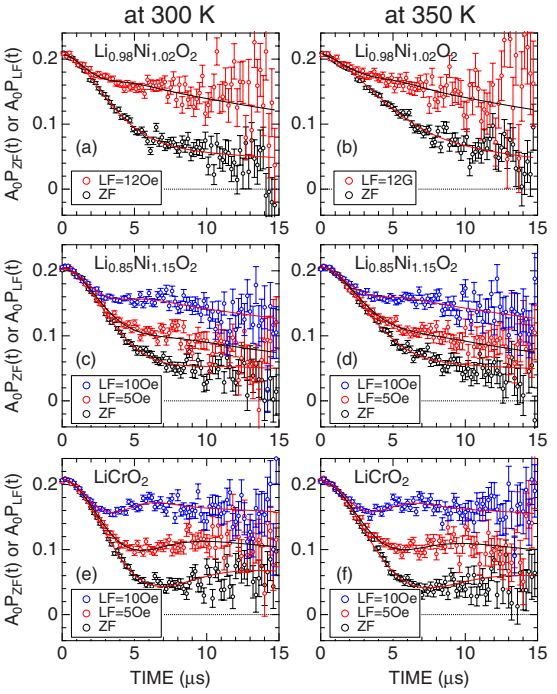

FIG. 6. (Color online) ZF- and two LF-μ^+SR spectra for [(a) and (b)] $Li_{0.98}Ni_{1.02}O_2$, [(c) and (d)] $Li_{0.85}Ni_{1.15}O_2$, and [(e) and (f)] $LiCrO_2$. (a), (c), and (e) were obtained at 300 K while (b), (d), and (f) at 350 K. Solid lines represent the fit result using Eq. (4). These spectra were obtained in J-PARC.

field (H_{int}^N) mainly caused by ^{6}Li and ^{7}Li. Figure 6 shows the ZF- and longitudinal-field-(LF) μ^+SR spectrum for the x =0.02 and 0.15 samples obtained at 300 K (left) and 350 K (right), together with those for $LiCrO_2$. Here, $LiCrO_2$ poses the same $R\bar{3}m$ crystal structure as $LiNiO_2$ but is electrochemically inactive,[44,45] i.e., Li^+ ions are not removed from the lattice by a usual electrochemical reaction. Preparation and characterization including μ^+SR measurements at low T for the $LiCrO_2$ sample were described in detail elsewhere.[43]

At 300 K, the ZF-spectrum exhibits a Kubo-Toyabe (KT) behavior with the change in the slope $[dP_{ZF}(t)/dt]$ around $t\sim 7\mu$s for $Li_{1-x}Ni_{1+x}O_2$ and a clear minimum around $t\sim 7\mu$s for $LiCrO_2$. The applied LF clearly reduces the relaxation rate, i.e., the time slope, by *decoupling* H_{int}^N. For $Li_{1-x}Ni_{1+x}O_2$, although the ZF spectrum still shows KT behavior at 350 K, the relaxation rate is smaller than at 300 K, indicating the increase in the field fluctuation rate (ν) with T. On the other hand, for $LiCrO_2$, the ZF and LF spectra at 350 K are eventually the same to those at 300 K. This means that H_{int}^N is static even at 350 K.

In order to estimate the KT parameters precisely, the ZF and LF spectra were fitted simultaneously by a combination of a dynamic Gaussian KT function $[G^{DGKT}(\Delta,\nu,t,H_{LF})]$ (Ref. 11) and an offset BG signal from the fraction of muons stopped mainly in the sample cell, which is made of high-purity titanium

$$A_0P_{LF}(t)=A_{KT}G^{DGKT}(\Delta,\nu,t,H_{LF})+A_{BG}, \quad (4)$$

where A_0 is the initial (t=0) asymmetry and A_{KT} and A_{BG} are the asymmetries associated with the two signals. Δ is the

static width of the local-field distribution at the disordered sites and ν is the field fluctuation rate. When $\nu=0$ and $H_{LF}=0$, $G^{DGKT}(t,\Delta,\nu,H_{LF})$ is the static Gaussian KT function $G_{zz}^{KT}(t,\Delta)$ in ZF. We fitted all the ZF and LF spectra using common A_{KT} and A_{BG} in the whole T range and common, i.e., H_{LF} independent, Δ and ν at each T in Eq. (4). The obtained A_{KT} and A_{BG} were 0.1518 ± 0.0001 and 0.0550 ± 0.0001 for $Li_{0.98}Ni_{1.02}O_2$, 0.1664 ± 0.0001 and 0.0398 ± 0.0002 for $Li_{0.85}Ni_{1.15}O_2$, and 0.1602 ± 0.0005 and 0.0397 ± 0.0007 for $LiCrO_2$.

Note that there is no longer a 1/3 tail term in Eq. (4) because the samples are in a paramagnetic state. In fact, the ZF and LF spectra above T_m for the three samples without the titanium cell were well fitted only by the KT signal. Also, it was confirmed that the ZF spectrum for the empty titanium cell exhibits a negligibly small relaxation, i.e., its exponential relaxation rate is $(0.0083\pm0.0004)\times10^6$ s^{-1} at 2 K and $(0.00066\pm0.0014)\times10^6$ s^{-1} at 150 K.

Figure 7 shows the T dependences of both Δ and ν for $Li_{1-x}Ni_{1+x}O_2$ and $LiCrO_2$. As T increases from 75 K, Δ for the $x=0.02$ sample decreases monotonically up to around 175 K, and then decrease slowly with T up to 400 K. The relatively rapid decrease in Δ with T in the T range between 75 and 175 K is most likely caused by electronic magnetism, as $T_m=18$ K for $Li_{0.98}Ni_{1.02}O_2$. In order to estimate the contribution of electron magnetism, we also attempted to fit the ZF and LF spectra by the exponentially relaxing dynamic KT function[8]

$$A_0P_{LF}(t)=A_{KT}G^{DGKT}(\Delta,\nu,t,H_{LF})\exp(-\lambda t)+A_{BG}. \quad (5)$$

Here, the $\exp(-\lambda t)$ term comes from the electronic fluctuations in the high-T regime, i.e., far above T_m. However, since $\lambda<10^{-1}$ s^{-1}, eventually 0, even at 75 K, such effect on Δ is too small to be distinguishable by a simple model for $Li_{0.98}Ni_{1.02}O_2$.

Above 175 K, the magnitude of Δ and its T dependence for the $x=0.02$ sample is very similar to those for the $x=0.15$ sample and $LiCrO_2$. This means that muons locate in the vicinity of the oxygen anions in both $Li_{1-x}Ni_{1+x}O_2$ and $LiCrO_2$ lattice, as predicted by electrostatic potential calculations. Furthermore, this indicates that Δ is determined mainly by Li, being consistent with the fact that the natural abundance for the NMR-active ^{61}Ni is 1.14%, that for ^{53}Cr is 9.5%, and that for ^{17}O is 0.038%, respectively. Although such Δ should, in principle, be T independent, the measured Δ slightly decreases with T, probably due to thermal expansion of the lattice—i.e., the increase in the distance between μ and Li. However, the $\Delta(T)$ curve only for the $x=0.02$ sample shows a sudden decrease above 400 K, indicating a motional narrowing by muon/Li diffusion.

In contrast to Δ, the $\nu(T)$ curve exhibits a clear sample dependence. That is, for $Li_{0.98}Ni_{1.02}O_2$, as T increases from 150 K, ν is almost T independent ($\sim0.2\times10^6$ s^{-1}) until 250 K, then, increases with T up to ~380 K, and then suddenly decreases with further increasing T. The $\nu(T)$ curve for $Li_{0.85}Ni_{1.15}O_2$ also exhibits a rapid increase with T above ~325 K. For $LiCrO_2$, on the other hand, ν is found to be almost T independent from 275 K to the highest T measured (475 K). This demonstrates that both μ^+s and Li^+ ions are

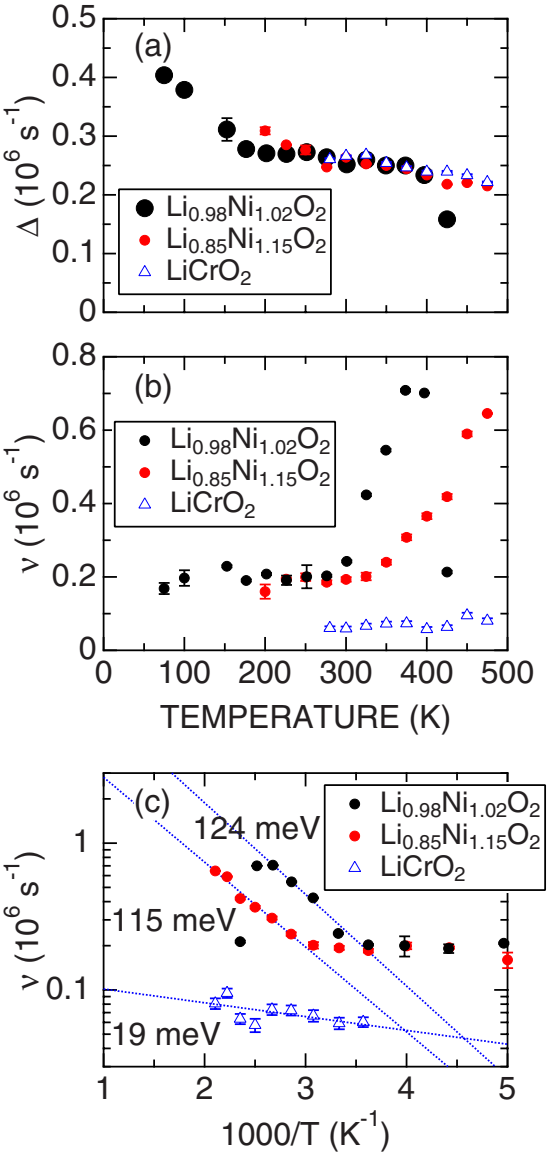

FIG. 7. (Color online) T dependences of (a) Δ and (b) ν for $Li_{1-x}Ni_{1+x}O_2$ with $x=0.02$ and 0.15, and $LiCrO_2$. (c) the relationship between ν and $1/T$. The data were obtained by global fitting the ZF and LF spectra using Eq. (4). The straight lines in (c) show the thermally activated behavior discussed in the text.

static in the $LiCrO_2$ lattice at least until 475 K. Since the muons are electrostatically bound to the oxygen anions, the implanted μ^+s in the $LiNiO_2$ lattice are also expected to be static up to around 475 K. Therefore, the origin of the increase in ν above 300 K (325 K) for $Li_{0.98}Ni_{1.02}O_2$ ($Li_{0.85}Ni_{1.15}O_2$) is reasonably assigned as Li diffusion. This is also consistent with our original assumption that D_{Li} decreases with x in $Li_{1-x}Ni_{1+x}O_2$ due to the hindrance of diffusion by the $(Ni)_{3b}$ ions in the Li^+ diffusion plane. Furthermore, only for $Li_{0.98}Ni_{1.02}O_2$, the $\nu(T)$ curve exhibits a clear maximum around 400 K, above which Δ suddenly decreases with T. This suggests that muons start to diffuse above ~400 K, resulting in the motional narrowing, as in the case for $Li_{0.73}CoO_2$ above ~300 K.[33]

TABLE II. D_{Li} and an activation energy (E_a) of ν estimated from the present μ^+SR measurements for $Li_{1-x}Ni_{1+x}O_2$ and $LiCrO_2$. The data for $Li_{0.73}CoO_2$ and $Li_{0.53}CoO_2$ are also listed for comparison.

Material	$Li_{0.98}Ni_{1.02}O_2$	$Li_{0.85}Ni_{1.15}O_2$	$LiCrO_2$	$Li_{0.73}CoO_2$	$Li_{0.53}CoO_2$
D_{Li} at 400 K (cm^2/s)	$4.70(3)\times10^{-11}$	$2.00(8)\times10^{-11}$			
D_{Li} at 350 K (cm^2/s)	$3.24(4)\times10^{-11}$	$0.63(8)\times10^{-11}$			
D_{Li} at 300 K (cm^2/s)	$0.39(3)\times10^{-11}$	$0.12(7)\times10^{-11}$		13.3×10^{-11} [a]	7.83×10^{-11} [a]
E_a (eV)	0.124	0.115	0.019	0.093[a]	0.098[a]

[a]See Ref. 7, but due to a numerical estimation error, the above D_{Li} values are correct.

2. Estimation of diffusion coefficient

In fact, the increase in ν for the $Li_{1-x}Ni_{1+x}O_2$ samples are well explained by a thermal activation process, $\nu \propto \exp(E_a/k_BT)$ [see Fig. 7(c)], as expected for the Li^+ diffusion. Here, E_a is the activation energy. Furthermore, since E_a for $LiCrO_2$ is about 1/10 of E_a for $Li_{1-x}Ni_{1+x}O_2$, the increase in ν for $LiCrO_2$ is likely caused by another mechanism, such as, an electron contribution. Assuming that ν corresponds to the jump rate of the Li^+ ions between the neighboring sites, D_{Li} is given by[46]

$$D_{Li} = \sum_{i=1}^{n} \frac{1}{N_i} Z_{v,i} s_i^2 \nu, \tag{6}$$

where N_i is the number of Li sites in the ith path, $Z_{v,i}$ is the vacancy fraction, and s_i is the jump distance. Here, the regular Li site is fully occupied by Li or Ni, we naturally consider only the jump to an interstitial site in the center of the oxygen tetrahedron.[4,7] Therefore, $i=1$, $N=3$, $s=a_H/\sqrt{3}$, and $Z=1$. Moreover, we assume that ν below 300 K is caused by the fluctuation of $3d$ electrons probably due to a dynamic Jahn-Teller (JT) effect of the Ni^{3+} ions in a low-spin state, as discussed later. Therefore, we estimated the average ν (ν_{ave}) using the data at $T \leq 275$ K at first, and then ν_{ave} was subtracted from the measured ν to calculate D_{Li} using Eq. (6). Here, $\nu_{ave}=0.201(6)\times10^6$ s^{-1} for $Li_{0.98}Ni_{1.02}O_2$ and $0.183(9)\times10^6$ s^{-1} for $Li_{0.85}Ni_{1.15}O_2$. The obtained D_{Li} and other parameters are summarized in Table II.

Based on Li-NMR measurements, it was reported that $D_{Li}^{NMR}=6\times10^{-15}$ cm^2/s for $LiNiO_2$ even at 500 K.[3] This value is clearly too small for cathode materials, and is probably because the NMR signal, i.e., spin-lattice relaxation rate, is artificially enhanced by the $3d$ electrons, as in the case for Li_xCoO_2 discussed earlier. On the other hand, D_{Li}^{EC} was estimated as $\sim1.2\times10^{-12}$ cm^2/s for $Li_{\sim1}NiO_2$ at 298 K (Ref. 47) from the chemical diffusion coefficient ($\tilde{D}_{Li}$), which was obtained by electrochemical measurements. Considering the difficulty of the estimation for the thermodynamic factor ($\Theta=\tilde{D}_{Li}/D_{Li}$), the reliability of D_{Li}^{EC} would be questionable. Unfortunately, there is no theoretical prediction for D_{Li} (D_{Li}^{calc}) of $LiNiO_2$. However since D_{Li}^{calc}(300 K) for $LiCoO_2$ (Ref. 4) agrees with D_{Li}^{EC} for $Li_{\sim1}NiO_2$, D_{Li} for $LiNiO_2$ is most likely on the order of 10^{-12} cm^2/s at 300 K. It is, therefore, reconfirmed that μ^+SR provides reasonable D_{Li} even for $Li_{1-x}Ni_{1+x}O_2$. Here, we also wish to mention that the increase in x strongly reduces D_{Li}, as expected.

The mass difference between μ^+ and Li^+ leads to the possibility that muons might diffuse with Li^+ at high T.[10] However, the estimated D_{Li} by μ^+SR is found to be comparable to D_{Li}^{EC}, as mentioned above. This means that the contribution of muon diffusion on D_{Li} is not predominant at least for the layered $LiMO_2$ (M=Cr, Co, and Ni) until a certain temperature, below which $\nu \propto \exp(1/T)$.

IV. DISCUSSION

A. Susceptibility anomaly around 300 K

For the $x=0.15$ sample, the $\chi^{-1}(T)$ curve deviates downwards from the linear relationship below ~300 K [see Fig. 1(b)]. This behavior was also reported by several groups by magnetization and electron-spin-resonance measurements.[22,24,25,37,41,48] Furthermore, such behavior was reported even for $Li_{0.98}Ni_{1.02}O_2$ under $H=10$ Oe.[37] In order to know the change in the microscopic magnetism for $Li_{0.85}Ni_{1.15}O_2$, Fig. 8 shows the T dependence of the wTF

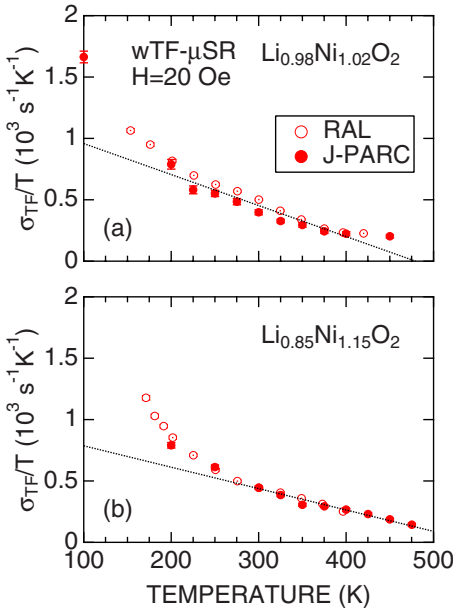

FIG. 8. (Color online) T dependences of σ_{TF}/T for (a) $Li_{0.98}Ni_{1.02}O_2$ and (b) $Li_{0.85}Ni_{1.15}O_2$. σ_{TF} was obtained by fitting the wTF spectra using a function, $A_{TF}\cos(\omega_{TF}^{\mu}t+\phi_{TF})\exp(-\sigma_{TF}^2t^2/2)$. Solid circles represent the data obtained in J-PARC while open circles in ISIS/RAL. Broken lines were obtained by linear fitting the data (a) between 225 and 400 K and (b) between 300 and 475 K.

Gaussian relaxation rate (σ_{TF}) divided by T. The data were obtained with wTF=20 Oe, which is the nuclear field (see Fig. 6).

A clear change in the slope around 200 K (250 K) can be seen more clearly in the plot of σ_{TF}/T vs T for the $x=0$ ($x=0.15$) sample. This indicates the change in the magnetic nature below 200 K (250 K) because σ_{TF} comes from the dipole interaction, In other words, since μ^+SR is a local probe and is not sensitive to magnetic impurities, the change observed in the $\chi^{-1}(T)$ curve around 300 K is found to be an intrinsic behavior for $Li_{0.85}Ni_{1.15}O_2$. The fact that the $\chi^{-1}(T)$ curve depends on H, in particular, at low H, usually suggests either the formation of ferromagnetic/ferrimagnetic order or the freezing of localized spins below 300 K. The former possibility was already excluded, because A_{TF} levels off at its maximum value above T_m [see Fig. 3(a)], demonstrating the absence of any kind of magnetic order, neither long ranged nor short ranged, above T_m for $Li_{1-x}Ni_{1+x}O_2$. For the latter case, a fast relaxation and/or a KT behavior due to $3d$ electron spins are expected to be observed in the ZF-μ^+SR spectra. Therefore, the latter possibility, i.e., a simple spin-glasslike freezing, is also eliminated by μ^+SR. We, thus, wish to propose that such an anomaly is induced by a dynamic Jahn-Teller distortion, as discussed in the next section.

B. Field fluctuation above T_m

One of the significant features of the $Li_{1-x}Ni_{1+x}O_2$ system above T_m is that $\nu \sim 0.2\times10^6$ cm^2/s and is T independent until $\sim$300 K($=T_d^{Li}$), at which the diffusion of the Li^+ ions is detectable [see Fig. 7(b)]. This behavior is very different from those for $LiCrO_2$ and Li_xCoO_2 (Refs. 5–7) for which $\nu < 0.1\times10^6$ cm^2/s below T_d^{Li}, despite the similarity of their crystal structures. Therefore, the origin of the large ν below T_d^{Li} is definitely thought to be caused by the Ni ions.

The related compound, $NaNiO_2$, is known to exhibit a structural phase transition from a high-T rhombohedral phase to a low-T monoclinic phase at $\sim$480 K (Ref. 49) due to a cooperative Jahn-Teller distortion of the Ni^{3+} ions with $S=1/2(t_{2g}^6e_g^1)$. In contrast to $NaNiO_2$, a similar structural phase transition has never been observed for $LiNiO_2$, while the magnetic anomaly was reported around 480 K. This could indicate the existence of a local JT distortion. However, a long-range cooperative JT distortion was never developed even at low T, probably due to the presence of JT inactive Ni^{2+} ions in the NiO_2 plane. Therefore, the observed ν between T_m and T_d^{Li} is most likely caused by the local JT distortion of the Ni^{3+} ions. This also indicates a dynamic nature of the local JT distortion that was pointed out a possibility in recent theoretical work.[50] Since such local JT distortion is coupled to the displacement of the coordinating oxygen ions, it is reasonable that the fluctuation rate of the local JT distortion is comparable to the jump rate of the Li^+ ions.

On the other hand, since the long-range cooperative JT distortion completes below 480 K for $NaNiO_2$,[49] the Ni^{3+} ions are expected to be static. Unfortunately, past μ^+SR work on $NaNiO_2$ concentrated the AF transition at $T_N=20$ K.[51] However, according to our preliminary μ^+SR experiment on $NaNiO_2$, $\nu \sim 0$ even at 100 K. This also supports our assumption that a dynamic local JT distortion is the origin of the relatively large ν below T_d^{Li} for $LiNiO_2$. This leads to the possibility for estimating T_d^{Li} more correctly. As seen in Fig. 7(c), at $1000/T < \sim 3.5$, log ν for $LiCrO_2$ is proportional to T^{-1} with a smaller slope than those for $LiNiO_2$. Assuming that ν for $LiCrO_2$ is a typical value for the static system with space group $R\bar{3}m$, we can estimate a real $T_d^{Li}(T_{d,real}^{Li})$ from the cross point of the two linear relationships, namely, $1000/T_{d,real}^{Li} \sim 4(T_{d,real}^{Li} \sim 250$ K) for $Li_{0.85}Ni_{1.15}O_2$ and $1000/T_{d,real}^{Li} \sim 4.6(T_{d,real}^{Li} \sim 217$ K) for $Li_{0.98}Ni_{1.02}O_2$. The estimated $T_{d,real}^{Li}$ agrees with the temperature, at which the $\sigma_{TF}/T(T)$ curve changes the slope (see Fig. 8). Since the Li diffusion naturally reduces the field distribution at the muon site(s), the estimated $T_{d,real}^{Li}$ is thought to be reasonable from the wTF measurements.

According to the theoretical work,[50] the dynamic JT distortion is induced by resonances between different states; for instance, between phase C and phase C', in which each Ni^{3+} ion forms a dimer singlet with its nearest-neighboring (NN) Ni^{3+} ion. In each dimer, the $d_{3z^2-r^2}$ orbital of one Ni ion is parallel to that of the other Ni ion. Furthermore, the dimers cover the triangular lattice. Due to the presence of Ni^{2+} ions and the coupling to the lattice,[52,53] the system would prefer to freeze so as to fill the triangular lattice with nonperiodic dimers.[31,50,54,55] This situation is likely to occur for $LiNiO_2$ at $T_m < T < T_d^{Li}$, resulting in a magnetic anomaly reported by magnetization measurements. At $T \geq T_d^{Li}$ (or $\nu \geq \nu_{ave}$), however, such dimer is expected to be very unstable, and eventually disappears due to the Li^+ diffusion because the reversible jump of the Li^+ ions reduces the local distortion of the NiO_2 plane in order to keep local charge neutrality. Consequently, we wish to propose that the dynamic local JT distortion is the origin of the magnetic anomaly at T_d^{Li} but the effect of such distortion on the magnetism is suppressed by Li^+ diffusion above T_d^{Li}.

C. Li diffusion in lithium transition-metal dioxides

Based on our μ^+SR measurements on $LiMO_2$ with M=Cr, Co, and Ni, their $T_{d,real}^{Li}$ were found to be 150 K for Li_xCoO_2 ($x=0.73$ and 0.53), 217–250 K for $Li_{1-x}Ni_{1+x}O_2$ ($x=0.02$ and 0.15), and above 475 K for $LiCrO_2$, respectively. Interestingly, the order of $T_{d,real}^{Li}$ looks to correlate with their electron-transport properties. That is, Li_xCoO_2 shows a metallic behavior,[6,56] $LiNiO_2$ is reported to show a semiconducting behavior,[57,58] and $LiCrO_2$ is an insulator.[59] Since the Li^+ ions are strongly bound to the NN oxygen anions in insulating materials, the Li^+ ions should be very stable even at high T—i.e., the Li^+ ions are not mobile. On the other hand, in metallic materials, $3d$ electrons no longer localized at the M ions but delocalized in the MO_2 plane. Hence, the binding energy between Li^+ and oxygen anions are weaker than that in insulating materials, resulting in mobile Li^+ in solids. This is a qualitative explanation on the order of $T_{d,real}^{Li}$ in $LiMO_2$. In other words, in order to predict the Li^+ diffusive behavior, we need precise calculations using a delocalized electron model plus electron-electron correlations, particularly to search for materials with high D_{Li}.

From the viewpoint of application of $LiNiO_2$ for Li-ion batteries, x is known to increase with the number of charge/discharge cycles. Such increase in x is thought to be one of the predominant reasons for capacity fading.[35] The present μ^+SR measurements have clarified that a small increase in x strongly reduces D_{Li}. For example, D_{Li} at 300 K for the $x=0.15$ sample is about a quarter of that for $x=0.02$ (see Table II). This unambiguously evidences the effect of x on the battery performance. Furthermore, wTF μ^+SR measurements provide information on the volume fraction of the phase with $x \geq 0.02$ through the normalized $A_{TF}(T)$ curve. This is because the normalized A_{TF} is roughly proportional to the volume fraction of paramagnetic phases in a sample, and T_m is sensitively dependent on x [see Fig. 3(d)]. Therefore, we believe that μ^+SR is a unique tool for developing positive electrode materials and investigating the capacity fading mechanism.

V. SUMMARY

We have investigated the low-T magnetism and high-T diffusive behavior of $Li_{1-x}Ni_{1+x}O_2$ with $x=0.02$, 0.03, and 0.15 by means of μ^+SR. From the low-T measurements, we have found: (1) a bulk FM transition for the $x=0.03$ and 0.15 samples while an AF transition for $x=0.02$ at 18 ± 4 K. (2) A clear increase in the FM transition temperature with x, namely, 48 ± 6 K for $x=0.03$ and 161 ± 7 K for $x=0.15$. (3) These results suggest a homogeneous change in the magnetic nature with x of the whole system rather than the formation of AF NiO-type domains or FM Ni-rich clusters.

Then, following upon the μ^+SR work on $LiCoO_2$ (Ref. 7) to determine its diffusion coefficient of Li^+ ions (D_{Li}), we have attempted to evaluate D_{Li} of $Li_{1-x}Ni_{1+x}O_2$ with $x=0.02$ and 0.15 together with $LiCrO_2$. The former material is heavily investigated as a positive electrode material of Li-ion batteries while the latter is electrochemically inactive. From the high-T measurements, we have found: (1) $D_{Li}(300\ K) \sim 0.39(3) \times 10^{-11}$ cm^2/s for $Li_{0.98}Ni_{1.02}O_2$ and $0.12(7) \times 10^{-11}$ cm^2/s for $Li_{0.85}Ni_{1.15}O_2$ but no diffusive behavior until at least 475 K for $LiCrO_2$. (2) These results are very consistent with the crystallographic nature and electrochemical properties of $Li_{1-x}Ni_{1+x}O_2$ and $LiCrO_2$. (3) A dynamic local Jahn-Teller distortion of the Ni^{3+} ions in a paramagnetic state of $Li_{1-x}Ni_{1+x}O_2$. Such distortion was detectable only at low temperatures, where Li^+ ions are static.

Finally, we emphasized the unique power of μ^+SR for the research of Li-ion batteries through D_{Li} measurements and paramagnetic volume fraction measurements.

ACKNOWLEDGMENTS

We thank the staff of J-PARC, ISIS, and TRIUMF for help with the μ^+SR experiments. We also thank the staff of SPring-8 for help with the XRD experiment, which was approved by the Japan Synchrotron Radiation Research Institute (Proposal No. 2008B1874). In addition, we thank K. Ariyoshi of Osaka City University for sample preparation and Y. Kondo of TCRDL for ICP-AES analysis. Y.I. and J.S. are partially supported by the KEK-MSL Inter-University Program for Oversea Muon Facilities, J.H.B. is supported at UBC by NSERC of Canada and (through TRIUMF) by NRC of Canada, and K.H.C. by NSERC of Canada and (through TRIUMF) by NRC of Canada. This work is also partially supported by Grant-in-Aid for Scientific Research (B), Grant No. 19340107 under MEXT, Japan.

*e0589@mosk.tytlabs.co.jp

[1] I. Tomeno and M. Oguchi, J. Phys. Soc. Jpn. **67**, 318 (1998).
[2] K. Nakamura, M. Yamamoto, K. Okamura, Y. Michihiro, I. Nakabayashi, and T. Kanashiro, Solid State Ionics **121**, 301 (1999).
[3] K. Nakamura, H. Ohno, K. Okamura, Y. Michihiro, I. Nakabayashi, and T. Kanashiro, Solid State Ionics **135**, 143 (2000).
[4] A. Van der Ven and G. Ceder, Electrochem. Solid-State Lett. **3**, 301 (2000).
[5] J. Sugiyama, H. Nozaki, J. H. Brewer, E. J. Ansaldo, G. D. Morris, and C. Delmas, Phys. Rev. B **72**, 144424 (2005).
[6] K. Mukai, Y. Ikedo, H. Nozaki, J. Sugiyama, K. Nishiyama, D. Andreica, A. Amato, P. L. Russo, E. J. Ansaldo, J. H. Brewer, K. H. Chow, K. Ariyoshi, and T. Ohzuku, Phys. Rev. Lett. **99**, 087601 (2007).
[7] J. Sugiyama, K. Mukai, Y. Ikedo, H. Nozaki, M. Månsson, and I. Watanabe, Phys. Rev. Lett. **103**, 147601 (2009).
[8] C. T. Kaiser, V. W. J. Verhoeven, P. C. M. Gubbens, F. M. Mulder, I. de Schepper, A. Yaouanc, P. Dalmas de R éotier, S. P. Cottrell, E. M. Kelder, and J. Schoonman, Phys. Rev. B **62**, R9236 (2000).
[9] M. J. Ariza, D. J. Jones, J. Rozière, J. S. Lord, and D. Ravot, J. Phys. Chem. B **107**, 6003 (2003).
[10] P. C. M. Gubbens, M. Wagemaker, S. Sakarya, M. Blaauw, A. Yaouanc, P. Dalmas de Réotier, and S. P. Cottrell, Solid State Ionics **177**, 145 (2006).
[11] R. S. Hayano, Y. J. Uemura, J. Imazato, N. Nishida, T. Yamazaki, and R. Kubo, Phys. Rev. B **20**, 850 (1979).
[12] G. M. Kalvius, D. R. Noakes, and O. Hartmann, in *Handbook on the Physics and Chemistry of Rare Earths*, edited by K. A. Gschneidner, Jr., L. Eyring, and G. H. Lander (North-Holland, Amsterdam, 2001), Vol. 32, Chap. 206.
[13] K. Nakamura, H. Ohno, K. Okamura, Y. Michihiro, T. Moriga, I. Nakabayashi, and T. Kanashiro, Solid State Ionics **177**, 821 (2006).
[14] M. G. S. R. Thomas, W. I. F. David, J. B. Goodenough, and P. Groves, Mater. Res. Bull. **20**, 1137 (1985).
[15] J. R. Dahn, U. von Sacken, and C. A. Michal, Solid State Ionics **44**, 87 (1990).
[16] J. R. Dahn, U. von Sacken, M. W. Juzkow, and H. Al-Janaby, J. Electrochem. Soc. **138**, 2207 (1991).
[17] C. Delmas, M. Ménétrier, L. Croguennec, S. Levasseur, J. P. Pérès, C. Puillerie, G. Prado, L. Fournès, and F. Weill, Int. J. Inorg. Mater. **1**, 11 (1999).
[18] R. Kanno, H. Kubo, Y. Kawamoto, T. Kamiyama, F. Izumi, Y. Takeda, and M. Takano, J. Solid State Chem. **110**, 216 (1994).

[19] T. Ohzuku, A. Ueda, and M. Nagayama, J. Electrochem. Soc. **140**, 1862 (1993).
[20] P. G. Bruce, Chem. Commun. **1997**, 1817.
[21] L. D. Dyer, B. S. Borie, and G. P. Smith, J. Am. Chem. Soc. **76**, 1499 (1954).
[22] K. Hirakawa, H. Kadowaki, and K. Ubukoshi, J. Phys. Soc. Jpn. **54**, 3526 (1985).
[23] M. Takano, R. Kanno, and T. Takeda, Mater. Sci. Eng., B **63**, 6 (1999).
[24] Y. Takahashi, J. Akimoto, Y. Gotoh, K. Kawaguchi, and S. Mizuta, J. Solid State Chem. **160**, 178 (2001).
[25] J. N. Reimers, J. R. Dahn, J. E. Greedan, C. V. Stager, G. Liu, I. Davidson, and U. Von Sacken, J. Solid State Chem. **102**, 542 (1993).
[26] A. Rougier, C. Delmas, and G. Chouteau, J. Phys. Chem. Solids **57**, 1101 (1996).
[27] J. B. Goodenough, D. G. Wickham, and W. J. Croft, Phys. Chem. Solids **5**, 107 (1958).
[28] M. J. Lewis, B. D. Gaulin, L. Filion, C. Kallin, A. J. Berlinsky, H. A. Dabkowska, Y. Qiu, and J. R. D. Copley, Phys. Rev. B **72**, 014408 (2005).
[29] K. Yamaura, M. Takano, A. Hirano, and R. Kanno, J. Solid State Chem. **127**, 109 (1996).
[30] Y. Kitaoka, T. Kobayashi, A. Koda, H. Wakabayashi, Y. Niino, H. Yamakage, S. Taguchi, K. Amaya, K. Yamaura, M. Takano, A. Hirano, and R. Kanno, J. Phys. Soc. Jpn. **67**, 3703 (1998).
[31] J.-H. Chung, Th. Proffen, S. Shamoto, A. M. Ghorayeb, L. Croguennec, W. Tian, B. C. Sales, R. Jin, D. Mandrus, and T. Egami, Phys. Rev. B **71**, 064410 (2005).
[32] A. J. W. Reitsma, L. F. Feiner, and A. M. Olés, New J. Phys. **7**, 121 (2005).
[33] J. Sugiyama, K. Mukai, Y. Ikedo, P. L. Russo, H. Nozaki, D. Andreica, A. Amato, K. Ariyoshi, and T. Ohzuku, Phys. Rev. B **78**, 144412 (2008).
[34] K. Mukai, J. Sugiyama, Y. Ikedo, P. L. Russo, D. Andreica, A. Amato, K. Ariyoshi, and T. Ohzuku, J. Power Sources **189**, 665 (2009).
[35] A. Rougier, P. Gravereau, and C. Delmas, J. Electrochem. Soc. **143**, 1168 (1996).
[36] F. Izumi and T. Ikeda, Mater. Sci. Forum **198**, 321 (2000).
[37] E. Chappel, M. D. Núñez-Regueiro, G. Chouteau, A. Sulpice, and C. Delmas, Solid State Commun. **119**, 83 (2001).
[38] E. Chappel, M. D. Núñez-Regueiro, S. de Brion, G. Chouteau, V. Bianchi, D. Caurant, and N. Baffier, Phys. Rev. B **66**, 132412 (2002).
[39] H. Ikeno, I. Tanaka, Y. Koyama, T. Mizoguchi, and K. Ogasawara, Phys. Rev. B **72**, 075123 (2005).
[40] L. C. Bartel and B. Morosin, Phys. Rev. B **3**, 1039 (1971).
[41] C. B. Azzoni, A. Paleari, V. Massarotti, M. Bini, and D. Capsoni, Phys. Rev. B **53**, 703 (1996).
[42] D. Andreica, Ph.D. thesis, IPP/ETH-Zurich, 2001.
[43] J. Sugiyama, M. Månsson, Y. Ikedo, T. Goko, K. Mukai, D. Andreica, A. Amato, K. Ariyoshi, and T. Ohzuku, Phys. Rev. B **79**, 184411 (2009).
[44] S.-T. Myung, S. Komaba, N. Hirosaki, N. Kumagai, K. Arai, R. Kodama, and I. Nakai, J. Electrochem. Soc. **150**, A1560 (2003).
[45] S. Komaba, C. Takei, T. Nakayama, A. Ogata, and N. Yabuuchi, Electrochem. Commun. **12**, 355 (2010).
[46] R. J. Borg and G. J. Dienes, *An Introduction to Solid State Diffusion* (Academic Press, San Diego, 1988).
[47] P. G. Bruce, A. Lisowska-Oleksiak, M. Y. Saidi, and C. A. Vincent, Solid State Ionics **57**, 353 (1992).
[48] P. Ganguly, V. Ramaswamy, I. S. Mulla, R. F. Shinde, P. P. Bakare, S. Ganapathy, P. R. Rajamohanan, and N. V. K. Prakash, Phys. Rev. B **46**, 11595 (1992).
[49] E. Chappel, M. D. Néñez-Regueiro, G. Chouteau, O. Isnard, and C. Darie, Eur. Phys. J. B **17**, 615 (2000).
[50] F. Vernay, K. Penc, P. Fazekas, and F. Mila, Phys. Rev. B **70**, 014428 (2004).
[51] P. J. Baker, T. Lancaster, S. J. Blundell, M. L. Brooks, W. Hayes, D. Prabhakaran, and F. L. Pratt, Phys. Rev. B **72**, 104414 (2005).
[52] M. V. Mostovoy and D. I. Khomskii, Phys. Rev. Lett. **89**, 227203 (2002).
[53] L. Petit, G. M. Stocks, T. Egami, Z. Szotek, and W. M. Temmerman, Phys. Rev. Lett. **97**, 146405 (2006).
[54] F. Reynaud, D. Mertz, F. Celestini, J.-M. Debierre, A. M. Ghorayeb, P. Simon, A. Stepanov, J. Voiron, and C. Delmas, Phys. Rev. Lett. **86**, 3638 (2001).
[55] E. Chappel, M. D. Néñez-Regueiro, F. Dupont, G. Chouteau, C. Darie, and A. Sulpice, Eur. Phys. J. B **17**, 609 (2000).
[56] M. Ménétrier, I. Saadoune, S. Levasseur, and C. Delmas, J. Mater. Chem. **9**, 1135 (1999).
[57] J. Molenda, P. Wilk, and J. Marzec, Solid State Ionics **119**, 19 (1999).
[58] J. Molenda, P. Wilk, and J. Marzec, Solid State Ionics **146**, 73 (2002).
[59] T. A. Hewston and B. L. Chamberland, J. Phys. Chem. Solids **48**, 97 (1987).